

## Soluble salt sources in medieval porous limestone sculptures: A multi-isotope (N, O, S) approach

Wolfram Kloppmann, Olivier Rolland, Anne-Thérèse Montech, Eric Proust

► **To cite this version:**

Wolfram Kloppmann, Olivier Rolland, Anne-Thérèse Montech, Eric Proust. Soluble salt sources in medieval porous limestone sculptures: A multi-isotope (N, O, S) approach. *Science of the Total Environment*, Elsevier, 2014, 470-471, pp.559-566. 10.1016/j.scitotenv.2013.09.087 . hal-00868337

**HAL Id: hal-00868337**

**<https://hal-brgm.archives-ouvertes.fr/hal-00868337>**

Submitted on 6 Nov 2013

**HAL** is a multi-disciplinary open access archive for the deposit and dissemination of scientific research documents, whether they are published or not. The documents may come from teaching and research institutions in France or abroad, or from public or private research centers.

L'archive ouverte pluridisciplinaire **HAL**, est destinée au dépôt et à la diffusion de documents scientifiques de niveau recherche, publiés ou non, émanant des établissements d'enseignement et de recherche français ou étrangers, des laboratoires publics ou privés.

1  
2  
3  
4 Soluble salt sources in medieval porous limestone  
5  
6  
7  
8 sculptures: A multi-isotope (N, O, S) approach.  
9

10  
11  
12  
13 *W. Kloppmann<sup>a\*</sup>, O. Rolland<sup>b</sup>, E. Proust<sup>a</sup>, A.T. Montech<sup>a</sup>*  
14

15  
16  
17 <sup>a</sup> BRGM, Direction des Laboratoires, Unité Isotopes, BP 6009, F-45060 Orléans cedex 2,  
18  
19 France, <sup>b</sup> Specialist in stone restoration, Montlouis-sur-Loire, France,  
20

21  
22 olivierrolland@wanadoo.fr  
23

24  
25 \* Corresponding author; e-mail: [w.kloppmann@brgm.fr](mailto:w.kloppmann@brgm.fr) BRGM  
26  
27

28  
29  
30 **Abstract**  
31

32  
33  
34  
35  
36 The sources and mechanisms of soluble salt uptake by porous limestone and the associated  
37  
38 degradation patterns were investigated for the life-sized 15<sup>th</sup> century “entombment of Christ”  
39  
40 sculpture group located in Pont-à-Mousson, France, using a multi-isotope approach on  
41  
42 sulfates ( $\delta^{34}\text{S}$  and  $\delta^{18}\text{O}$ ) and nitrates ( $\delta^{15}\text{N}$  and  $\delta^{18}\text{O}$ ). The sculpture group, near the border of  
43  
44 the Moselle River, is within the potential reach of capillary rise from the alluvial aquifer.  
45  
46 Chemical analyses show a vertical zonation of soluble salts with a predominance of sulphates  
47  
48 in the lower parts of the statues where crumbling and blistering prevail, and higher  
49  
50 concentrations of nitrates and chloride in the high parts affected by powdering and  
51  
52 efflorescence. Isotope fingerprints of sulphates suggest a triple origin: (1) the lower parts are  
53  
54 dominated by capillary rise of dissolved sulphate from the Moselle water with characteristic  
55  
56  
57  
58  
59  
60  
61  
62  
63  
64  
65

1 Keuper evaporite signatures that progressively decreases with height; (2) in the higher parts  
2 affected by powdering the impact of atmospheric sulphur becomes detectable; and (3) locally,  
3  
4 plaster reparations impact the neighbouring limestone through dissolution and re-precipitation  
5  
6  
7 of gypsum. Nitrogen and oxygen isotopes ~~of nitrates~~ suggest an organic origin of nitrates of in  
8  
9 all samples. N isotope signatures are compatible with those measured in the alluvial aquifer of  
10  
11 the Moselle River further downstream. This indicates contamination by sewage or organic  
12  
13 fertilizers. Significant isotopic contrasts are observed between the different degradation  
14  
15 features depending on the height and suggest historical changes of nitrate sources.  
16  
17  
18  
19  
20

21 **Keywords:** stone degradation, sulphate, nitrate, capillary rise, cultural heritage, isotope  
22  
23 fingerprinting, sulphur, oxygen, nitrogen.  
24  
25  
26  
27

## 28 **1. Historical and environmental context**

29  
30 The “Entombment of the Christ” is a recurrent motive of French statuary of the 15<sup>th</sup> and 16<sup>th</sup>  
31  
32 century (Forsyth, 1970). The studied group in St. Martin’s Church in Pont-à-Mousson, North-  
33  
34 eastern France (Figure 1, Figure 1S, Supplementary Information) is supposed to have been  
35  
36 ordered for the funerary monument of Baldemar-Johannis of Biebelnheim and executed  
37  
38 between 1425 and 1430 (Karsallah, 2009, Fréchet, 1991) supposedly by an east-European  
39  
40 artist. The group of sculptures comprises 13 standing or lying life-size statues and 8 smaller  
41  
42 statues of angles suspended at the vault. It is likely that the present day emplacement is the  
43  
44 historical one even if important modifications in the 19<sup>th</sup> century are reported (partial  
45  
46 replacement of the soldier group, De Sansonetti 1844). The last restoration campaign took  
47  
48 place in 1973. This campaign was limited to replacing lost parts and ignored soluble salts as  
49  
50 the principal cause of those losses. The gradual evolution of salt degradation can be followed  
51  
52 from the very first photographs around 1900. As early in 1844, the text by de Sansonetti  
53  
54 (1844) stated that “the group is more damaged by frost than by man” which has to be  
55  
56  
57  
58  
59  
60  
61  
62  
63  
64  
65

1 interpreted in the light of the fact that before the last quarter of the twentieth century damages  
2 due to salts were often attributed to frost or to wind erosion.  
3

4 The original material of the sculptures is a fine-grained limestone; some recent  
5 replacements are made of oolitic limestone (summit of the cross, elbow of the second female  
6 saint). Several reparations and replacements made use of gypsum plaster. The monument has  
7 alterations of different types (ICOMOS, 2008): disintegration and superficial cracks,  
8 powdering in the higher parts, efflorescences (chemical precipitates), and fragmentation  
9 (Figure 1).  
10  
11  
12  
13  
14  
15  
16  
17  
18

19 The church is situated in the direct vicinity (50 m) of the Moselle River around 3 m above  
20 mean base level. The statues are in contact, directly or indirectly via a mortar layer, with a soil  
21 made of calcareous dressed stone or, in some places, made of a compacted mix of earth and  
22 calcareous stone fragments. This soil is visibly porous and hydrophilic but its basic properties  
23 are unknown. Spots of humidity on the soil elsewhere in the church indicate capillary rise.  
24  
25  
26  
27  
28  
29  
30

31 Alluvial aquifers are generally hydraulically connected to the river; it is therefore likely that  
32 accompanying groundwater has similar contents of major ions especially during high-flow  
33 conditions where river water inflow predominates compared to local recharge. Supplementary  
34 input of nitrates is possible via the sewer network and diffuse agricultural pollution but the  
35 decomposition of human corpses in tombs can also play a role as nitrogen source (WHO,  
36 1998). Dissolved ions may contribute to the degradation of the “Entombment of the Christ”  
37 through capillary rise of groundwater. Air pollution is another source of soluble salts and has  
38 been strong in the past as witnessed by thick black crusts on the Southern facade of the  
39 church. Air pollution is mainly a source of sulphates, to a much lesser extent of nitrates and  
40 chlorides. Air pollution mainly affects the exterior of buildings but also, to a minor but still  
41 measurable extent, their interior (e.g. Kramar *et al.*, 2011). Indeed, Pont à Mousson became,  
42 from 1856 onward, the most important centre of cast iron tube production in France with up  
43  
44  
45  
46  
47  
48  
49  
50  
51  
52  
53  
54  
55  
56  
57  
58  
59  
60  
61  
62  
63  
64  
65

1 to five blast furnaces in activity, reduced to two in 2009 and one in 2011. Other factors of  
2 local air pollution are heavy car traffic and a nearby thermal power plant (DRIRE, 2004).  
3  
4 Gypsum plaster reparations which have been identified in several places (Rolland, 2012)  
5  
6 represent a supplementary risk of sulphate contamination (Kloppmann *et al.*, 2011, Vallet *et*  
7  
8 *al.*, 2006), in particular in the context of capillary rise which may lead to dissolution,  
9  
10 mobilisation and recrystallization of the calcium sulphates which constitute gypsum plaster.  
11  
12

13  
14 The present multi-isotope study is part of the pre-restoration assessment currently  
15  
16 conducted by O. Rolland on account of the DRAC (Regional Division of Cultural Affairs)  
17  
18 Lorraine. The choice of the isotope tracers, employed in the aim of elucidating sources and  
19  
20 mechanisms of weathering, was guided by the nature of the observed soluble salts.  
21  
22 Preliminary investigations found mainly sulphates and nitrates with some chlorides, so we  
23  
24 combined  $\delta^{34}\text{S}$  and  $\delta^{18}\text{O}_{(\text{SO}_4)}$  with  $\delta^{15}\text{N}$  and  $\delta^{18}\text{O}_{(\text{NO}_3)}$  with the aim of constraining the sources  
25  
26 of soluble salts inducing different types of alteration. Curiously enough, given the widespread  
27  
28 occurrence of both Na- and K-nitrate salts (nitre, nitratine), alums and Ca-, Mg-, Na-sulphates  
29  
30 in building stones (mainly gypsum, thenardite, mirabilite, hexahydrate and epsomite, Flatt,  
31  
32 2002), this combination of tools has, to our knowledge, never been applied before. There is a  
33  
34 long record of isotope studies using  $\delta^{34}\text{S}$  signatures of black crusts and other alteration  
35  
36 features of building stones and sculptures since the early works in Salt Lake City (Dequasie  
37  
38 and Grey, 1970), Venice (Longinelli and Bartelloni, 1978), and Prague (Šrámek, 1980; Buzek  
39  
40 and Šrámek, 1985; Buzek *et al.*, 1991; for a more complete bibliography refer to Kloppmann  
41  
42 *et al.*, 2011, and Sanjurjo-Sanchez & Alves, 2012). The ambiguity of mono-isotope studies  
43  
44 (overlap of signatures of a large diversity of sources) can be overcome by combining several  
45  
46 tracers. After rare precursor studies in Venice (Longinelli and Bartelloni, 1978), and Antwerp  
47  
48 (Torfs *et al.*, 1997), recent works on stone decay combine oxygen and sulphur isotopes in  
49  
50 sulphate to discriminate pollution sources in urban environment (Vallet *et al.*, 2006,  
51  
52  
53  
54  
55  
56  
57  
58  
59  
60  
61  
62  
63  
64  
65

1 Schweigstillova *et al.*, 2009, Schleicher and Hernandez, 2010, Kloppmann *et al.*, 2011). Less  
2 “traditional” isotopes have been recently combined with sulphur and oxygen, like boron  
3  
4 (Kloppmann *et al.*, 2011) giving hints to the relative role of air pollution (coal combustion),  
5  
6 and sea-salts on monument in a coastal setting. Strontium and sulphur isotopes were  
7  
8 analysed together in salt efflorescences degrading the Angkor monuments and indicated bat  
9  
10 guano as main source of salts (sulphates, phosphates, carbonates, Hosono *et al.*, 2006). Lead  
11  
12 and strontium isotopes were combined (Åberg *et al.*, 1999) to investigate the role of traffic in  
13  
14 the degradation of Norwegian rock carvings. Steelman *et al.*, (2002) is a rare example for the  
15  
16 use of nitrogen isotopes in stone degradation studies. Using nitrogen combined with carbon  
17  
18 isotopes they revealed animal origin of black crusts on cave paintings in Idaho.  
19  
20  
21  
22  
23

24 We hypothesized use of the constituent isotopes of the observed nitrate and sulphate salts  
25  
26 would provide better constraints for disentangling the potential pollution sources impacting  
27  
28 the sculpture group. Our sampling strategy focused on the different degradation features,  
29  
30 including disintegration, powdering and efflorescences, and on the supposed contamination  
31  
32 end members: (1) Black crusts which can be considered as representative of air pollution and  
33  
34 integrating the pollution signal over long periods (Camuffo *et al.*, 1983; Ausset *et al.*, 1998,  
35  
36 Kloppmann *et al.*, 2011), (2) Moselle water potentially contributing salts from its dissolved  
37  
38 load through capillary rises, and (3) gypsum plaster used abundantly for reparations as  
39  
40 potential sulphate source.  
41  
42  
43  
44  
45  
46  
47

## 48 **2. Materials and Methods**

### 49 **2.1. Sampling**

50  
51 Sampling was limited to the surface of the degraded parts of the limestone, by superficial  
52  
53 scraping of the disintegrated parts and brushing of the disintegrated powdering parts and of  
54  
55 efflorescences (Figure 1). A grab sample of River water was taken on June 17, 2011 on the  
56  
57  
58  
59  
60  
61  
62  
63  
64  
65

1 right bank of the Moselle 20 cm below the surface close to the bridge in the vicinity of St.  
2 Martin's Church. .  
3

## 4 **2.2. Analytical methods**

5  
6 After crushing of the solid samples, nitrates and sulphates were solubilised by lixiviation  
7 with 250 ml of Millipore® highly distilled water over 72 h on an agitation table. Lixivates  
8 are then filtered at 0.45 µm. Chemical composition was then determined by Inductively  
9 coupled plasma atomic emission spectroscopy (ICP-AES, Horiba Ultima 2) for major cations  
10 and ion chromatography (Cl<sup>-</sup>, NO<sub>3</sub><sup>-</sup>, SO<sub>4</sub><sup>2-</sup>, limits of quantification: 0.5 mg/L) or titration  
11 (HCO<sub>3</sub><sup>-</sup>, limits of quantification limit 5 mg/L) for major anions. All chemical analyses follow  
12 international standard procedures (NF EN ISO/CEI 17025 : 2005).  
13  
14  
15  
16  
17  
18  
19  
20  
21  
22

23 The isotopic compositions are expressed in the usual delta notation as a per mil (‰)  
24 deviation of the heavy-to-light isotope abundance ratio (<sup>34</sup>S/<sup>32</sup>S, <sup>18</sup>O/<sup>16</sup>O, and <sup>15</sup>N/<sup>14</sup>N) in the  
25 sample from an international standard, sulphur isotopes as δ<sup>34</sup>S with respect to the CDT  
26 standard, oxygen isotopes as δ<sup>18</sup>O with respect to the SMOW, nitrogen isotopes with respect  
27 to the AIR standard.  
28  
29  
30  
31  
32  
33  
34  
35

36 **Sulphur and oxygen isotopes of sulphates;** For sulphur and oxygen isotope ratio  
37 determination lixivate was filtered at 0.22 µm and acidified before adding BaCl<sub>2</sub>. The  
38 precipitate of BaSO<sub>4</sub> is then recovered on a 0.45 µm filter, dried at 60°C for at least one night.  
39  
40  
41  
42

43 *Sulphur:* 300 µg of BaSO<sub>4</sub> is mixed with V<sub>2</sub>O<sub>5</sub> in a tin capsule. The capsule is then  
44 introduced in the elemental analyser (Flash EA) and the BaSO<sub>4</sub> reduced to SO<sub>2</sub> at 900°C. The  
45 SO<sub>2</sub> gas, purified by gas chromatography is then analysed on a Thermo Scientific  
46 DELTAplus XP continuous flow mass spectrometer (CF-IRMS).  
47  
48  
49  
50  
51  
52

53 *Oxygen:* A 200 µg aliquot of the previously obtained BaSO<sub>4</sub> in a silver capsule are injected  
54 into a graphite pyrolysis oven at 1450°C. The oxygen reacts with the graphite and forms CO  
55  
56  
57  
58  
59  
60  
61  
62  
63  
64  
65

1 gas which is, after purification by gas chromatography, analysed by CF-IRMS (DELTAplus  
2 XP).

3  
4 The standard analytical error between duplicate analyses is lower than  $\pm 0.3$  ‰ for  
5 both sulphur and oxygen.  
6  
7

8  
9  
10  
11 **Nitrogen and oxygen isotopes of nitrates:** The lixivate was purified by several  
12 subsequent steps of ion exchange and precipitation of chlorides, carbonates, sulphates and  
13 phosphates by adding AgCl and BaCl<sub>2</sub> (modified after Chang *et al.*, 1999, Silva *et al.*, 2000).  
14  
15 Solid nitrates are then obtained as AgNO<sub>3</sub> by lyophilisation.  
16  
17

18  
19 The solid AgNO<sub>3</sub> in a silver capsule is then injected in a graphite pyrolysis oven at 1450°C.  
20  
21 The gases obtained (CO and N<sub>2</sub>) are separated by gas chromatography and analysed  
22 successively by CF-IRMS (Thermo Scientific DELTA V).  
23  
24

25 All samples were measured as duplicates with a standard analytical error of lower than  
26 0.5 ‰.  
27  
28

### 29 **3. Results and Discussion**

#### 30 **3.1. Chemistry of soluble salts**

31  
32 Major ions (Table 2, providing solid/solid concentrations of the leachable fraction of the  
33 total rock), with exception of bivalent cations (Ca, Mg) and bicarbonates, which are related to  
34 the mineralogical nature of the limestone used for the group of sculptures, discriminate  
35 several types of alteration. Disintegrated stones without powdering (PA1, 3, 5) from the base  
36 of the statues are rich in sulphates (concentrations higher than 40 mg/g) but poor in Na, K,  
37 NO<sub>3</sub>, and Cl. Powdering stones from the upper parts of the statues are rather low in sulphates,  
38 with exception of sample PA7, but contain significant amounts of K, Na, NO<sub>3</sub><sup>-</sup>, and Cl which  
39 are more or less correlated (Figure 2). Efflorescences are mainly KNO<sub>3</sub> with negligible  
40 concentrations of other elements so that they plot outside the tendencies observed for the  
41 altered stone samples. Sample EF1 is somewhat richer compared to sample EF2 in sulphates  
42  
43  
44  
45  
46  
47  
48  
49  
50  
51  
52  
53  
54  
55  
56  
57  
58  
59  
60  
61



1 and chlorides (25 mg/g and 4 mg/g respectively, Figure 2). Both the black crust CN1 and the  
2 plaster of Paris PL1 contained more than 50% calcium sulphate;  
3

4 The water sample from the Moselle river, taken in November 2010 (Table 2) is quite rich in  
5 chloride (400 mg/L) and sulphates (113 mg/L) compared to the typical calcium-bicarbonate  
6 waters from catchments mainly built of carbonate rocks (median values for sulphate  
7 concentrations on French carbonate rock catchments range from 10 to 48 mg/L, whereas Cl  
8 concentrations corrected for precipitations are nil (cf. Meybeck, 1986). This is due to the  
9 presence of Triassic evaporites upstream of Pont-à-Mousson containing gypsum and halite  
10 (Brenot *et al.*, 2010). Nitrate and potassium contents were, on the contrary, quite low at the  
11 moment of sampling (3.4 and 1 mg/L respectively). The river water could therefore represent  
12 an important source of sulphates and chlorides, via groundwater and capillary rise. It has to be  
13 stated that nitrate concentrations in the river, mainly related to agricultural activities, are  
14 bound to vary strongly over the year (a range of 0.7 to 15 mg/L has been measured at Pont St.  
15 Vincent from March 2002 to September 2003, Brenot *et al.*, 2007). Supplementary input is  
16 possible directly into the alluvial aquifer (sewage, agricultural pollution) leading to higher  
17 concentrations. Up to 104 mg/L of nitrate were measured in the alluvial groundwater body  
18 accompanying the Moselle at Yutz (Widory and Nguyen-Thé, 2006). Thus, the measured  
19 Moselle water is very rich in sulphate and chloride, less in nitrates but the concentrations  
20 could be highly variable over the year.  
21  
22  
23  
24  
25  
26  
27  
28  
29  
30  
31  
32  
33  
34  
35  
36  
37  
38  
39  
40  
41  
42  
43  
44  
45  
46  
47

48 Spatial patterns of soluble salt concentrations as well as the identified alteration types vary  
49 in function of height (Figure 1). Close to the base of the statues, stones are disintegrated but  
50 not powdering; they are rich in sulphates and calcium, pointing to gypsum as main mineral,  
51 but low in nitrates and chlorides. In the higher parts, the sculptures are disintegrated and  
52 powdering, rich in chlorides, nitrates, sodium, and potassium. Chlorides represent a good  
53  
54  
55  
56  
57  
58  
59  
60  
61  
62  
63  
64  
65

1 tracer of Moselle water and of the accompanying alluvial groundwater as it can be expected  
2 that atmospheric inputs are not a significant source of chloride in a continental context.  
3  
4 Regional rainwater has in fact chloride concentrations < 3 mg/L in the studied zone (Blum *et*  
5 *al.*, 2002). The influence of river water/groundwater is perceptible for all sampling points but  
6  
7 concentrations of chlorides and nitrates are higher in the upper parts of the statues. Less  
8  
9 soluble salts (calcium sulphates) precipitate first during capillary rise whereas more soluble  
10  
11 salts (nitrates and chlorides) stay mobile and crystallise later, leading to the formation of  
12  
13 efflorescence and powdering. Such a zonation has been reported for stone monuments  
14  
15 concerned by capillary rise (Arnold, 2004)  
16  
17  
18  
19  
20

### 21 **3.2. Sulphur and oxygen isotopes of sulphates**

22 Potential sources of sulphates including air pollution, Moselle water, and groundwater, as  
23  
24 well as gypsum plasters used for reparations may be distinguished isotopically (Table 2). As  
25  
26 the origin and geological age of the limestone material used for the sculptures is not known, it  
27  
28 is difficult to estimate *a priori* the potential isotopic signatures of carbonate associated  
29  
30 sulfates (CAS) and sulphides that may give rise to sulphate formation. Measurements were  
31  
32 impossible as this would have implied drilling into non-altered material. However, no  
33  
34 macroscopic observation of sulphide oxidation was made (e.g. FeIII-hydroxides) and CAS  
35  
36 concentrations in chemically precipitated micritic limestones, as probably used for the  
37  
38 sculptures, are generally low (few tens of ppm, Kampschulte & Strauss, 2004 and references  
39  
40 therein) so that their impact can be considered as minor.  
41  
42  
43  
44  
45  
46  
47

48 The sulphates which constituted the major part of the black crust CN1 (37% of sulphate or  
49  
50 67% of gypsum), sampled on the external wall of the southern facade are considered as  
51  
52 representative of local air pollution as the sampling location was potentially out of reach of  
53  
54 capillary rise and no gypsum plaster was used in the surroundings. Their isotopic composition  
55  
56  
57  
58 with a  $\delta^{34}\text{S}$  of 0.8 ‰ vs. CDT and a  $\delta^{18}\text{O}$  of 8.5 ‰ vs. SMOW ~~falling~~falls indeed in the  
59  
60  
61  
62  
63  
64  
65

1 relatively narrow range typical for air pollution-derived black crusts measured on other  
2 French monuments out of the coastal zone potentially influenced by sea salts (Bourges and  
3 Chartres cathedrals, Chenonceau and Versailles castles, Kloppmann *et al.*, 2011) (Figure 3).  
4

5 Moselle water (E1) falls, with a  $\delta^{34}\text{S}$  of 13.6 ‰ and a  $\delta^{18}\text{O}$  of 12.3 ‰, in the field of Upper  
6 Triassic evaporites (Pearson *et al.*, 1991). This composition is similar to the range of values  
7 measured for Moselle water 45 to 50 km upstream from Pont-à-Mousson (Pont St. Vincent,  
8 Messein, Brenot *et al.*, 2007). Moselle water contains significant sulphate concentrations (113  
9 mg/L for our sample) due to the fact that Upper Triassic (Keuper) evaporites outcrop in some  
10 upstream parts of the Moselle catchment. They are dissolved by runoff and within the  
11 groundwater bodies which in turn feed tributaries and the Moselle River.  
12  
13  
14  
15  
16  
17  
18  
19  
20  
21  
22  
23

24 The gypsum plaster sample (PL1) is the sample which is most enriched in  $^{34}\text{S}$  and  $^{18}\text{O}$  with  
25 a  $\delta^{34}\text{S}$  of 17.2 ‰ and a  $\delta^{18}\text{O}$  of 22.6 ‰. It falls in the range of  $\delta^{34}\text{S}$  values measured for the  
26 Tertiary (Lutetian and Ludian) gypsum of the Paris basin (Fontes and Letolle, 1976, Fontes  
27 and Nielsen, 1966; Fontes and Thoulemont, 1987) but shows a slightly higher  $\delta^{18}\text{O}$ . Most  
28 gypsum plasters, commonly referred to as “Paris plaster” show in fact the isotope signature of  
29 Tertiary gypsum from the town of Paris (Kloppmann *et al.*, 2011). For CAS of Jurassic age,  
30  $\delta^{34}\text{S}$  values of 14.2 to 18 ‰ could be expected (Kampschulte & Strauss, 2004) in the same  
31 range as observed for the plaster endmember.  
32  
33  
34  
35  
36  
37  
38  
39  
40  
41  
42  
43

44 All stone samples fall clearly off a mixing line for  $\delta^{18}\text{O}$  and  $\delta^{34}\text{S}$  of the atmospheric and  
45 the plaster endmember. We observe two mixing trends requiring a third endmember which is  
46 compatible with mean Moselle water at Messein and Pont-St-Vincent ( $\delta^{34}\text{S} = 11.1$  ‰ and  
47  $\delta^{18}\text{O} = 13$  ‰). Nevertheless, the approximate co-linearity of the three end members makes it  
48 difficult to quantify their respective contributions (Figure 3). The disintegrated stone samples  
49 close to the base of the statues (PA1, 3, 5) fall in the field of Keuper gypsum, confirming the  
50 influence of groundwater through capillary rise (Figure 3). Samples of powdering stone taken  
51  
52  
53  
54  
55  
56  
57  
58  
59  
60  
61  
62  
63  
64  
65

1 on the upper parts of the statues (PA2, 4, 6, 8) show a good correlation ( $r^2=0.93$ ,  $n=4$ , [p-](#)  
2 [value=0.036](#) , [statistics performed with XLSTAT software package](#)) in the  $\delta^{34}\text{S}$  vs.  $\delta^{18}\text{O}$   
3  
4  
5 diagram (Figure 3) suggesting mixing between two end members, “Moselle water” and “air  
6  
7 pollution” represented respectively by samples E1 and CN1. Sulphates in sample PA4 appear  
8  
9 to be nearly exclusively dominated by air pollution. Indoor sulfation of carbonates can be  
10  
11 favoured by particulate matter (Grau-Bové and Strlic, 2013), itself containing oxidised  
12  
13 sulphur compounds (e.g. for diesel particulate matter) or acting as catalyser of  $\text{SO}_2$  fixation,  
14  
15 and gypsum formation (Roriguez-Navarro and Sebastian, 1996, Cultrone et al., 2008). It  
16  
17 needs to be stated, though, that this group of powdering stone samples is rather poor in  
18  
19 sulphates (0.4 to 16 mg/g). The powdering sample PA7 presents a singularity as it is shifted  
20  
21 towards the signature of the plaster sample PL1 and is rich in sulphates (>45 mg/L). It was  
22  
23 taken from the back of John (Mary and John are carved in a single bloc; Figure 1 and  
24  
25 Supplemental Information Photograph) in the vicinity of the plaster reparation which  
26  
27 provided PL1 and may contain plaster-derived sulphates, dissolved by capillary rising  
28  
29 groundwater, and then transported by diffusion in the interstitial porosity of the fine-grained  
30  
31 limestone.

32  
33  
34  
35  
36  
37  
38  
39 Sample PA9 taken from the external wall of the St. Martin church at the base of the  
40  
41 northern facade of the north tower is, isotopically speaking, very close to the black crust of  
42  
43 the southern facade and shows a predominance of atmospheric sulphates, in spite of its  
44  
45 proximity to the soil and the obvious signs of capillary rise at the sampling spot (Figure 3). It  
46  
47 seems that the strong environmental pressure from local air pollution (smelters) dominates  
48  
49 sulphate formation at the exterior of the building.

50  
51  
52  
53 Salt efflorescences at the internal wall of the chapel hosting the sculpture group (sample  
54  
55 EF1) contained enough sulphates (26 mg/g) to allow for isotope analysis of sulphates. Their  
56  
57 signature is very close to the black crust, suggesting atmospheric origin for the sulphate  
58  
59  
60  
61  
62  
63  
64  
65

1 contents of the efflorescences which are weak (5 to 26 mg/g) compared to nitrate (472 to 482  
2 mg/g).  
3

4 It is likely that isotope signatures of neoformed sulphates in the stone samples reflect  
5 closely those of dissolved sulphate in the pore water as isotope fractionation accompanying  
6 precipitation of solid sulphates is low ( $< +2$  ‰ enrichment in  $^{34}\text{S}$  of the solid phase in most  
7 studies, Raab & Spiro, 1999 and references therein, around  $+3.5$  ‰ enrichment in  $^{18}\text{O}$ ,  
8 Claypool *et al.*, 1980), lower than the potential variability of the end members (e.g. Moselle  
9 water: range of  $4.2$  ‰ for  $\delta^{18}\text{O}$  and of  $3.3$  ‰ for  $\delta^{34}\text{S}$ , Brenot *et al.* 2006). Oxygen isotope  
10 composition of sulphate can be expected to be stable over time as water-sulphate equilibrium  
11 exchange at ambient temperatures will take  $>10^7$  years (Chiba and Sakai, 1985).  
12  
13  
14  
15  
16  
17  
18  
19  
20  
21  
22  
23

24 Judging from the isotopic composition of sulphates of the “Entombment of the Christ” we  
25 can derive the following conclusions on their origin: Sulphates contained in the altered parts  
26 at the base of the statues show the influence of Moselle water or of river-derived groundwater  
27 in the alluvial aquifer, dominated by the dissolution of Keuper gypsum in the upstream parts  
28 of the catchment. The influence of river water can be explained by capillary rise of  
29 groundwater, in particular during high-water conditions that lead to rising groundwater levels.  
30 During the winter months the total sulphate concentrations will be lowered by dilution and the  
31 relative contribution of agricultural input increased (Brenot *et al.*, 2007). The powdering  
32 alteration in the higher parts of the statues falls between Moselle water and the “air pollution”  
33 endmember represented by the black crust CN1. The highest sample (PA4, female saint above  
34 the right breast) reveals to be closest to the atmospheric endmember. The influence of  
35 capillary rise is visible, for sulphate salts, up to the mid-height of the statues due to  
36 preferential precipitation of gypsum in the lower parts and overrides to varying extents the  
37 atmospheric signatures. Air pollution seems to have impacted the statues in spite of their  
38 sheltered situation in the interior of the church which can be explained by the strong local  
39  
40  
41  
42  
43  
44  
45  
46  
47  
48  
49  
50  
51  
52  
53  
54  
55  
56  
57  
58  
59  
60  
61  
62  
63  
64  
65

1 environmental pressure of metal industry and car exhausts. Indeed, the outdoor samples fall in  
2 the range of  $\delta^{34}\text{S}$  values reported for “pure” car traffic sulphur by Torfs *et al.*, (1997) between  
3  
4 -2.1 ‰ and +2.8 ‰. Gypsum plaster reparations constitute a significant source of calcium  
5 sulphate with a relatively limited spatial range of influence via dissolution, transport by  
6  
7 diffusion or capillarity and reprecipitation at the stone surface.  
8  
9

### 10 11 12 **3.3. Nitrogen and oxygen isotopes in nitrates** 13

14 As Moselle water (E1) could not be analysed for nitrogen and oxygen isotopes in nitrates  
15 due to the very low concentrations (2.8 mg/L), values for Moselle catchment are provided by  
16 the report of Widory and Nguyen-Thé (2006) who determined  $\delta^{15}\text{N}$  of the alluvial  
17 groundwater of the Moselle at Yutz, situated around 60 km further downstream. The reported  
18 values are highly variable, between 4.3 ‰ and 22 ‰ (n=4), samples with high  $\text{NO}_3^-$  showing  
19  $\delta^{15}\text{N}$  in the lower range (4.3 to 6.7 ‰). The variability of signatures is explained by the  
20 variability of nitrate sources, mainly mineral fertilisers and animal or human faeces (via  
21 sewage and organic fertilisers).  
22  
23  
24  
25  
26  
27  
28  
29  
30  
31  
32  
33

34 The analysed black crust CN1 was too low in nitrate to be analysed isotopically so that we  
35 lack the pure “air pollution” endmember for nitrate. In fact, “air pollution nitrate”, if present  
36 in the chapel, would not be expected to be concentrated in black crusts. In fact, black crust  
37 formation is strongly linked to sulphur oxides and distribution of airborne nitrogen deposits  
38 would be probably very different from those of sulphates.  $\delta^{15}\text{N}$  values of  $\text{NO}_x$  compounds,  
39 derived from coal combustion show isotope ratios similar to modern urban atmospheric  
40 particles, ranging from 5 to 13 ‰ (Heaton, 1987, Kiga *et al.*, 2000, Widory, 2007).  
41 References on  $\delta^{18}\text{O}$  of particle-bound nitrates are rather rare (Elliot *et al.*, 2009) and much  
42 higher than those encountered in our study. Gaseous  $\delta^{18}\text{O}_{\text{HNO}_3}$  and particle-bound  $\delta^{18}\text{O}_{\text{NO}_3}$  fall  
43 between 45 and 94 ‰ due to the role of ozone, strongly enriched in  $^{18}\text{O}$ , in the oxidation of  
44 nitrogen (Elliot *et al.*, 2009). To our knowledge, no reference exists on nitrogen and oxygen  
45  
46  
47  
48  
49  
50  
51  
52  
53  
54  
55  
56  
57  
58  
59  
60  
61  
62  
63  
64  
65

1 isotopes in altered calcareous building stones and the mechanisms of NO<sub>x</sub> oxidation, and  
2 interactions with ozone, SO<sub>x</sub>, and limestone are complex (Massey, 1999).  
3

4 The isotope signatures of nitrates (Table 2) differentiate two groups of disintegrated stone  
5 samples at the base of the statues (PA1, 3, 5) fall in a restricted range of δ<sup>15</sup>N values from 5.7  
6 to 6.3 ‰. The signatures of the most nitrate-rich alluvial groundwaters at Yutz (Widory and  
7 Nguyen-Thé, 2006) are compatible with those measured at the lower part of the statues. The  
8 efflorescences EF1 and EF2 as well as sample PA9, sampled at the external wall of the church  
9 within the potential zone of capillary rise, show a δ<sup>15</sup>N somewhat enriched in <sup>15</sup>N ranging  
10 from 7.3 to 9.5 ‰ (Figure 4). The disintegrated powdering stone samples from the upper part  
11 of the statues (PA2, 4, 8) form a well-defined group with a δ<sup>15</sup>N between 11.6 and 12.3 ‰,  
12 and δ<sup>18</sup>O between 5.4 and 8.9 ‰. Since measured δ<sup>18</sup>O<sub>(NO<sub>3</sub>)</sub> values are incompatible with an  
13 atmospheric origin of nitrates as they are much too low compared with the range of air  
14 pollution derived NO<sub>3</sub> (Elliot *et al.*, 2009) this indicates that the predominant agents of air  
15 pollution in the sector were SO<sub>x</sub> which is compatible with contamination from smelters.  
16  
17  
18  
19  
20  
21  
22  
23  
24  
25  
26  
27  
28  
29  
30  
31  
32  
33

34 Nitrates from all altered stone samples as well as the K-nitrate efflorescences fall in the  
35 field of animal waste (Figure 4, Kendall *et al.*, 2007) and are comparable to the signatures  
36 measured in the alluvial aquifer of the Moselle river further downstream. The nitrate contents  
37 of the altered stones seems therefore to stem from human faeces or animal waste, either via  
38 local sewage input or diffuse agricultural pollution of the riverine water by manure spreading  
39 in the upstream parts of the catchment. The fact that the measured Moselle water is richer in  
40 Na than in K is not incompatible with the preferential formation of nitre (KNO<sub>3</sub>) in the  
41 efflorescences as solubility of nitre is by a factor of 2 (at 20°C) to 4 (at 0°C) lower than that of  
42 nitratine (NaNO<sub>3</sub>) so that nitre will form first (Laue, 2005).  
43  
44  
45  
46  
47  
48  
49  
50  
51  
52  
53  
54  
55

56 We were not able to analyse the gypsum plaster sample given the low nitrate contents.  
57 Gypsum plaster could be *a priori* an important source of sulphates due to its chemical  
58  
59  
60  
61  
62  
63  
64  
65

1 composition ( $\text{CaSO}_4 \cdot 2\text{H}_2\text{O}$ ) but is unlikely to deliver much nitrate given the low measured  
2 concentrations (6.2 mg/g in PL1). Even though, as nitrates are easily leachable and very  
3 mobile, the initial nitrate contents of PL1 could have been diminished by dissolution and  
4 diffusion. Point PA9 (altered stone at the exterior wall of the North tower) shows capillary  
5 rise as main source of nitrates whereas its sulphate signatures indicate the impact of air  
6 pollution.  
7  
8  
9  
10  
11  
12

13 On the whole, it is therefore likely that all nitrates are derived from capillary rise contrarily to  
14 sulphates where three sources have been identified (capillary rise, air pollution and gypsum  
15 plaster leaching).  
16  
17  
18  
19  
20

21 The observed range in isotopic values of nitrates in the alluvial aquifer are too low to  
22 associate a distinct origin of nitrate salts with the different types of degradation  
23 (efflorescences, powdering, disintegration) or to the location of the samples (upper and lower  
24 parts of the statues). The reasons for the clumping of data for specific materials in Figure 4 is  
25 not totally clear. One hypothesis might be a succession of contamination with slightly  
26 different sources (eg. contribution of mineral fertilisers in the alluvial aquifer).  
27  
28  
29  
30  
31  
32  
33  
34  
35

#### 36 **4. Conclusions and recommendations**

37  
38 Chemical major ion analyses ( $\text{Cl}$ ,  $\text{NO}_3$ ,  $\text{SO}_4$ ,  $\text{Na}$ ,  $\text{K}$ ,  $\text{Mg}$ ) of the soluble fraction in the  
39 decayed parts of limestone sculptures highlight a clear differentiation between the  
40 disintegrated but not powdering stone at the base of the statues and the upper parts where  
41 stones show powdering. Lower parts, mainly impacted by disintegration, are rich in gypsum  
42 but contain low nitrates and chlorides. Powdering stones are rich in chlorides, nitrates, sodium  
43 and potassium. Since Moselle water has high sulphate and chloride, and variable nitrate  
44 concentrations this trend in major ion concentrations indicates that capillary rise via the  
45 alluvial aquifer can contribute to the salt contents even in the higher parts of the statues.  
46  
47  
48  
49  
50  
51  
52  
53  
54  
55  
56  
57  
58  
59  
60  
61  
62  
63  
64  
65



1  
2  
3  
4  
5  
6  
7  
8  
9  
10  
11  
12  
13  
14  
15  
16  
17  
18  
19  
20  
21  
22  
23  
24  
25  
26  
27  
28  
29  
30  
31  
32  
33  
34  
35  
36  
37  
38  
39  
40  
41  
42  
43  
44  
45  
46  
47  
48  
49  
50  
51  
52  
53  
54  
55  
56  
57  
58  
59  
60  
61  
62  
63  
64  
65

Neoformation of sulphates in the “Entombment of the Christ” group has a triple origin: (1) Moselle water contained in the alluvial aquifer in the disintegrated and powdering stones due to capillary rise, (2) air pollution which is superposed on the other sources and becomes progressively predominant in the higher parts less rich in sulphate, (3) dissolution of gypsum plaster used for restorations.

Nitrates are likely to be brought into the system by groundwater contaminated by sewage or diffuse agricultural pollution (isotope signature of “organic waste” type). Sepulchres with decomposed human material might also explain part of the observed saltpetre. The origin of the slight but significant differences between the isotope signatures of the different types of alteration is not fully elucidated. They could be historical resulting from successive pollution phases. Atmospheric input is not significant for the nitrate balance in the decayed parts of the sculptures. Isotope signatures of nitrates are less conclusive than S and O isotopes in our study as there is one predominating (organic) nitrate source. In another, multi-source context they may be more discriminating.

From a practical point of view, the restoration strategy has to include hydraulic isolation of the statues from the soil. Plaster reparations should be eliminated as they contribute locally to the neoformation of sulphates. The impact of air pollution is detectable but appears less important than the other soluble salt sources. As the industrial activity in the area has significantly decreased, this contamination pathway may be considered as historical.

### **Acknowledgements**

This study was supported by the DRAC Lorraine and co-financed by the Research Division of BRGM. We wish to warmly thank Veronique Verges-Belmin and Lise Leroux from LRMH (Laboratoire de Recherche des Monuments Historiques, Champs sur Marne, France) for fruitful discussions on the manuscript.

### **5. Bibliography**

1  
2  
3 Åberg G, Stray H, Dahlin E. Impact of Pollution at a Stone Age Rock Art Site in Oslo,  
4 Norway, Studied using Lead and Strontium Isotopes. *Journal of Archaeological Science*  
5 1999; 26: 1483-1488.  
6  
7

8  
9  
10  
11 Arnold A. Evolution des sels solubles dans l'altération et la conservation des monuments.  
12 Enduits dégradés par les sels : pathologies et traitements. ICOMOS-France, report Dossier  
13 Technique n°6-2004, 2004.  
14  
15  
16

17  
18  
19 Ausset P, Bannery F, Del Monte M, Lefevre RA. Recording of pre-industrial atmospheric  
20 environment by ancient crusts on stone monuments. *Atmospheric Environment* 1998; 32:  
21 2859-2863.  
22  
23  
24

25  
26  
27 Blum A, Chery L, Babrier J, Baudry D, Petelet-Giraud E, Ruppert N, et al. Contribution à la  
28 caractérisation des états de référence géochimique des eaux souterraines. Outils et  
29 méthodologie. Rapport final, report BRGM/RP-51549-FR, 2002.  
30  
31  
32  
33

34  
35  
36 Brenot A, Carignan J, France-Lanord C, Benoit M. Geological and land use control on delta  
37 S-34 and delta O-18 of river dissolved sulfate: The Moselle river basin, France. *Chemical*  
38 *Geology* 2007; 244: 25-41.  
39  
40  
41

42  
43  
44 Buzek F, Cerny J, Sramek J. Sulphur isotope studies of atmospheric S and the corrosion of  
45 monuments in Prague, Czechoslovakia. In: Krouse HR, Grinenko VA, editors. *Stable*  
46 *isotopes, natural and anthropogenic sulphur in the environment*. Wiley and Sons, Chichester,  
47 1991, pp. 399-405.  
48  
49  
50  
51

52  
53  
54 Buzek F, Šrámek J. Sulphur isotopes in the study of stone monument conservation. *Studies*  
55 *in Conservation*. *Studies in Conservation* 1985; 30: 171-176.  
56  
57  
58  
59  
60  
61  
62

1 Camuffo D, Delmonte M, Sabbioni C. Origin and growth mechanisms of the sulfated crusts  
2 on urban limestone. *Water Air and Soil Pollution* 1983; 19: 351-359.  
3

4  
5 Chang CCY, Langston J, Riggs M, Campbell DH, Silva SR, Kendall C. A method for  
6 nitrate collection for  $\delta^{15}\text{N}$  and  $\delta^{18}\text{O}$  analysis for water with low nitrate concentrations.  
7  
8 *Canadian Journal of Fisheries and Aquatic Sciences* 1999; 56: 1856-1864.  
9

10  
11  
12 Chiba H, Sakai H. Oxygen isotope exchange-rate between dissolved sulfate and water at  
13 hydrothermal temperatures. *Geochimica Et Cosmochimica Acta* 1985; 49: 993-1000.  
14  
15

16  
17  
18 Cultrone G, Arizzi A, Sebastian E, Rodriguez-Navarro C. Sulfation of calcitic and dolomitic  
19 lime mortars in the presence of diesel particulate matter. *Environmental Geology* 2008; 56:  
20  
21  
22  
23  
24 741-752  
25

26  
27 de Sansonetti V. Description de l'ancienne église des Antonistes maintenant paroisse Saint-  
28 Martin de Pont-à-Mousson. Nancy: Grimblot, Raybois et Cie, Imprimeurs-Libraires, 1844.  
29

30  
31  
32 Dequasie HL, Grey DC. Stable isotopes applied to pollution studies. *American Laboratory*  
33  
34  
35  
36 1970; 2: 19-27.  
37

38  
39 DRIRE. Environnement Industriel en Lorraine - Bilan 2004 - Perspectives 2005. La  
40  
41  
42 pollution de l'air. DRIRE, report, 2004.  
43

44  
45 Elliott EM, Kendall C, Boyer EW, Burns DA, Lear GG, Golden HE, et al. Dual nitrate  
46  
47  
48 isotopes in dry deposition: Utility for partitioning  $\text{NO}_x$  source contributions to landscape  
49  
50  
51 nitrogen deposition. *Journal of Geophysical Research-Biogeosciences* 2009; 114.  
52

53  
54 Flatt RJ. Salt damage in porous materials: how high supersaturations are generated. *Journal*  
55  
56  
57  
58  
59  
60  
61  
62  
63  
64  
65  
66 of Crystal Growth 2002; 242: 435-454.

1 Fontes JC, Letolle R. O-18 and S-34 in Upper Bartonian gypsum deposits of Paris basin.  
2 Chemical Geology 1976; 18: 285-295  
3

4  
5 Fontes JC, Nielsen H. Isotopes de l'oxygène et du soufre dans le gypse parisien. C.R. Acad.  
6 Sc. Paris Serie D 1966; 262: 2685-2687.  
7

8  
9  
10 Fontes J-C, Toulemont M. Facies, pétrologie et teneurs en isotopes lourds 18O, 13C, 34S  
11 des niveaux évaporitiques lutétiens supérieurs du bassin de Paris : Interprétation  
12 paléohydrologique. Bull. Centres Rech. Explor.-Prod. Elf-Aquitaine 1987; 11: 39-64.  
13  
14  
15

16  
17  
18 Forsyth WJ. The entombment of Christ. French sculptures of the fifteenth and sixteenth  
19 centuries. Cambridge (Massachussetts): Harvard University Press, 1970.  
20  
21

22  
23  
24 Fréchet G. La Mise au tombeau de l'église Saint-Martin de Pont-à-Mousson (ancienne  
25 commanderie des Antonins). Bulletin de la Société de l'Histoire de l'Art français 1991; 1991:  
26 9-20.  
27  
28  
29

30  
31  
32  
33  
34  
35  
36  
37  
38  
39  
40  
41  
42  
43  
44  
45  
46  
47  
48  
49  
50  
51  
52  
53  
54  
55  
56  
57  
58  
59  
60  
61  
62  
63  
64  
65

Grau-Bove J, Strlic M. Fine particulate matter in indoor cultural heritage: a literature  
review. Heritage Science 2013; 1: 8.

Heaton THE. 15N/14N ratios of NOx from vehicle engines and coal-fired power stations.  
Tellus Series B-Chemical and Physical Meteorology 1990; 42: 304- 307.

Holser WT, Kaplan IR, Sakai H, Zak I. Isotope geochemistry of oxygen in the sedimentary  
sulfate cycle. Chemical Geology 1979; 25: 1-17.

Hosono T, Uchida E, Suda C, Ueno A, Nakagawa T. Salt weathering of sandstone at the  
Angkor monuments, Cambodia: identification of the origins of salts using sulfur and  
strontium isotopes. Journal of Archaeological Science 2006; 33: 1541-1551.

1 ICOMOS-ISCS Illustrated glossary on stone deterioration patterns = Glossaire illustré sur  
2 les formes d'altération de la pierre. English-French version - Version Anglais-Français.  
3  
4 Verges-Belmin V. ed. Paris: ICOMOS-ISCS, 2008. 78 p. (Monuments and Sites; XV). ISBN:  
5 978-2-918086-00-0.  
6  
7  
8  
9

10 Kampschulte A, Strauss H. The sulfur isotopic evolution of Phanerozoic seawater based on  
11 the analysis of structurally substituted sulfate in carbonates. *Chemical Geology* 2004; 204:  
12 255-286.  
13  
14  
15  
16  
17

18 Karsallah E. Les Mises au tombeau monumentales du Christ en France (XVe-XVIe siècles):  
19 enjeux iconographique, funéraire et dévotionnel. Thèse de doctorat. Université de Paris IV,  
20 2009, pp. 362.  
21  
22  
23  
24  
25

26 Kendall C, Elliott EM, Wankel SD. Tracing Anthropogenic Inputs of Nitrogen to  
27 Ecosystems. In: Lajtha K, Michener RH, editors. *Stable Isotopes in Ecology and*  
28 *Environmental Science* 2nd ed. Blackwell Scientific Publications, 2007.  
29  
30  
31  
32  
33

34 Kloppmann W, Bromblet P, Vallet JM, Verges-Belmin V, Rolland O, Guerrot C, et al.  
35 Building materials as intrinsic sources of sulphate: A hidden face of salt weathering of  
36 historical monuments investigated through multi-isotope tracing (B, O, S). *Science of the*  
37 *Total Environment* 2011; 409: 1658-1669.  
38  
39  
40  
41  
42  
43  
44

45 Kramar S, Mirtic B, Knoeller K, Rogan-Smuc N. Weathering of the black limestone of  
46 historical monuments (Ljubljana, Slovenia): Oxygen and sulfur isotope composition of sulfate  
47 salts. *Applied Geochemistry* 2011; 26: 1632-1638.  
48  
49  
50  
51  
52

53 Laue S. Salt Weathering of Porous Structures Related to Climate Changes. *Restoration of*  
54 *Buildings and Monuments/Bauinstandsetzen und Baudenkmalpflege* 2005; 11: 381-390.  
55  
56  
57  
58  
59  
60  
61  
62

1 Longinelli A, Bartelloni M. Atmospheric pollution in Venice, Italy, as indicated by isotope  
2 analyses. Water Air and Soil Pollution 1978; 10: 335-341.  
3

4  
5 Massey SW. The effects of ozone and NO<sub>x</sub> on the deterioration of calcareous stone. Science  
6 of the Total Environment 1999; 227: 109-121.  
7

8  
9  
10  
11 Meybeck M. (1986) Composition chimique des ruisseaux non pollués de France. Sci. Geol.  
12 Bull. 39, 3-77.  
13

14  
15  
16  
17 Nguyen-Thé D, Widory D. Etude isotopique de l'origine des nitrates dans l'aquifère  
18 calcaire situé entre l'Aire et la Cousances (Meuse). BRGM, report BRGM/RP-54410-FR,  
19 2006, pp. 38.  
20  
21

22  
23  
24  
25 Pearson FJ, Balderer J, W., Loosli HH, Lehmann BE, Matter A, Peters T, et al. Applied  
26 isotope hydrology - A case study in Northern Switzerland edited by. Studies in Environmental  
27 Sciences. Vol. 43. Elsevier Science Publishers B.V., Amsterdam-London-New York-Tokyo,  
28 1991, pp. 460.  
29  
30  
31

32  
33  
34  
35 Raab M, Spiro B. Sulfur isotopic variations during seawater evaporation with fractional  
36 crystallization. Chemical Geology 1991; 86: 323-333.  
37

38  
39  
40  
41 RodriguezNavarro C, Sebastian E. Role of particulate matter from vehicle exhaust on  
42 porous building stones (limestone) sulfation. Science of the Total Environment 1996; 187: 79-  
43 91.  
44  
45  
46

47  
48  
49 Sanjurjo-Sanchez J, Alves C. Decay effects of pollutants on stony materials in the built  
50 environment. Environmental Chemistry Letters 2012; 10: 131-143.  
51  
52  
53  
54  
55  
56  
57  
58  
59  
60  
61  
62

1 Schleicher N, Hernandez CR. Source identification of sulphate forming salts on sandstones  
2 from monuments in Salamanca, Spain-a stable isotope approach. Environmental Science and  
3  
4 Pollution Research 2010; 17: 770-778.  
5  
6

7  
8 Schweigstillova J, Prikryl R, Novotna M. Isotopic composition of salt efflorescence from  
9 the sandstone castellated rocks of the Bohemian Cretaceous Basin (Czech Republic).  
10 Environmental Geology 2009; 58: 217-225.  
11  
12  
13

14  
15  
16 Silva SR, Kendall C, Wilkinson DH, Ziegler AC, Chang CCY, Avanzino RJ. A new method  
17 for collection of nitrate from fresh water and the analysis of nitrogen and oxygen isotope  
18 ratios. Journal of Hydrology 2000; 228: 22-36.  
19  
20  
21  
22

23  
24 Šrámek J. Determination of the source of surface deterioration of surface deterioration of  
25 tombstones at the old Jewish cemetery in Prague. Studies in Conservation 1980; 25: 47-52.  
26  
27  
28

29  
30 Steelman K, Rowe MW, Boutton TW, Southon JR, Merrel CL, Hill RD. Stable Isotope and  
31 Radiocarbon Analyses of a Black Deposit associated with Pictographs at Little Lost River  
32 Cave, Idaho. J. Archaeological Sci. 2002; 19: 1189-1198.  
33  
34  
35  
36

37  
38 Torfs KM, Van Grieken RE, Buzek F. Use of Stable Isotope Measurements To Evaluate the  
39 Origin of Sulfur in Gypsum Layers on Limestone Buildings. Environmental Science &  
40 Technology 1997; 31: 2650-2655.  
41  
42  
43  
44

45  
46 Vallet JM, Gosselin C, Bromblet P, Rolland O, Verges-Belmin V, Kloppmann W. Origin of  
47 salts in stone monument degradation using sulphur and oxygen isotopes: First results of the  
48 Bourges cathedral (France). Journal of Geochemical Exploration 2006; 88: 358-362.  
49  
50  
51  
52

53  
54 Verges-Belmin V. Deterioration of Stone in Monuments. In: Schrefler B, Delage P, editors.  
55 Environmental Geomechanics. John Wiley & Sons, 2010, pp. 201-245.  
56  
57  
58  
59  
60  
61  
62

1 WHO. The impact of cemeteries on the environment and public health. WHO report  
2 EUR/ICP/EHNA 01 04 01(A), 1998.  
3  
4

5 Widory D. Nitrogen isotopes: Tracers of origin and processes affecting PM10 in the  
6 atmosphere of Paris. Atmospheric Environment 2007; 41: 2382-2390.  
7  
8  
9

10 Widory D, Nguyen-Thé D. Etude isotopique de l'origine des nitrates dans la nappe alluviale  
11 de la Moselle dans le secteur de Yutz (Moselle). BRGM, report BRGM/RP-54409-FR, 2006,  
12 pp. 34.  
13  
14  
15  
16  
17  
18  
19  
20  
21  
22  
23  
24  
25  
26  
27  
28  
29  
30  
31  
32  
33  
34  
35  
36  
37  
38  
39  
40  
41  
42  
43  
44  
45  
46  
47  
48  
49  
50  
51  
52  
53  
54  
55  
56  
57  
58  
59  
60  
61  
62  
63  
64  
65



## Figure captions

1  
2 Figure 1: Mapping of alteration types and superficial deposits (modified after Rolland, 2012).  
3 The brown patches are places where the surface of the sculpture is covered with a brownish  
4 natural patina. Examples of the two main degradation features are provided with powdering  
5 (above) and disintegration (below). Arrows indicate sampling points for isotope analyses  
6 (rear= rear surface of the statue)  
7

8  
9 Figure 2: Chemical contents of solid samples (altered stones, efflorescences and plaster) in the  
10 Saint Martin church of Pont-à-Mousson.  
11

12 Figure 3: Isotopes signatures ( $\delta^{34}\text{S}$  vs.  $\delta^{18}\text{O}$ ) of black crusts, altered stones, efflorescences  
13 and plaster in the Saint Martin church of Pont-à-Mousson. For comparison: gypsum crusts in  
14 Antwerpen (Torfs et al., 1997), Venice (Longinelli et Bartelloni, 1978) and different French  
15 inland monuments (Kloppmann et al., 2011), Keuper aquifer groundwaters (Pearson et al.,  
16 1991), Mosel river water at Pont St. Vincent and Messein 45-50 km upstream of Pont-à-  
17 Mousson (Brenot et al., 2007) and atmospheric oxygen.  
18  
19

20 Figure 4: Isotopes signatures ( $\delta^{15}\text{N}$  vs.  $\delta^{18}\text{O}$ ) of black crusts, altered stones, efflorescences and  
21 plaster in the Saint Martin church of Pont-à-Mousson. Fields of  $\delta^{18}\text{O}$  and  $\delta^{15}\text{N}$  of nitrates  
22 originating from atmospheric sources, soils, mineral and organic fertilisers and sewage (after  
23 Kendall et al., 2007)  
24  
25

26 Supplementary Information Figure 1S: General view of the « Entombment of the Christ » group  
27 in the Saint Martin church of Pont-à-Mousson (photo : O. Rolland); inserted map of France  
28 with situation of Pont-à-Mousson  
29  
30

## Table captions

31  
32  
33  
34  
35 Table 1: Samples of pollution sources and altered stones  
36

37 Table 2: Major ion and isotopic analyses on stone and river samples with standard analytical  
38 errors  
39  
40  
41  
42  
43  
44  
45  
46  
47  
48  
49  
50  
51  
52  
53  
54  
55  
56  
57  
58  
59  
60  
61  
62  
63  
64  
65

*Table 1: Samples of pollution sources and altered stones*

Sample	Description	Emplacement
CN1	Black crust	Exterior of the chapel, southern facade, eastern pilaster, base of the solid arched bay
E1	Moselle water	Moselle river, right shore near the bridge, 20 cm below surface
EF1	Efflorescence	Eastern wall behind the purse of Joseph of Arimathea
EF2	Efflorescence	Interior of the right sleeve of Joseph of Arimathea
PA1	Disintegrated stone without powdering	Below the folds between the feet of Joseph of Arimathea
PA2	Powdering disintegrated stone	Below the right breast of the holy woman rising her right hand
PA3	Disintegrated stone without powdering	Under the base of the tombstone, southern surface, eastern edge
PA4	Powdering disintegrated stone	Below the right breast of the holy woman rising her right hand
PA5	Disintegrated stone without powdering	Under the lower edge of the gown of Nicodemus, fold nearest to the eastern leg of the funerary table
PA6	Powdering disintegrated stone	Right lower part of the back of Mary
PA7	Powdering disintegrated stone	Back of Saint John
PA8	Powdering disintegrated stone	Veil of Mary below the right breast
PA9	Disintegrated stone without powdering	North tower, northern facade, near the basis.
PL1	Gypsum Plaster	Back of Saint John

Table 2 : Major ion and isotopic analyses on stone and river samples with standard analytical errors

Sample	Ca	Mg	Na	K	HCO <sub>3</sub>	Cl	SO <sub>4</sub>	NO <sub>3</sub>	$\delta^{34}\text{S}$	$\delta^{18}\text{O}$	$\delta^{15}\text{N}$	$\delta^{18}\text{O}$
	mg/g total	mg/g total	mg/g total	mg/g total	mg/g total	mg/g total	mg/g total	mg/g total	‰ vs. CDT	‰ vs. SMO (SO <sub>4</sub> ) W	‰ vs. AIR	‰ vs. SMO (NO <sub>3</sub> ) W
	± 5%	± 5%	± 5%	± 5%	± 5%	± 5%	± 5%	± 5%	± 0.3 ‰	± 0.3 ‰	± 0.5 ‰	± 0.5 ‰
CN1	156,5	0,2	0,6	0,5	3,8	0,8	371,1	1,6	0,8	8,5	nd	nd
EF1	15,4	0,2	0,8	263,5	3,7	4,1	25,6	472,5	0,4	8,9	7,3	8,7
EF2	6,9	0,6	0,6	273,6	18,1	1,3	5,0	482,1	nd	nd	9,5	3,8
PA1	16,5	0,2	0,1	0,5	0,6	0,3	> 39*	3,5	11,2	14,8	5,7	9,9
PA2	5,8	0,1	3,2	2,2	1,1	2,9	11,5	10,4	7,8	11,4	12,3	8,9
PA3	28,5	0,5	0,2	0,3	1,7	0,2	>70*	2,7	12,8	13,9	5,9	11,3
PA4	4,2	0,1	3,8	2,4	2,6	3,0	6,6	12,2	4,1	8,4	11,8	8,2
PA5	20,3	0,3	0,4	0,6	0,6	0,2	> 50*	5,1	13,7	16,7	6,3	12,8
PA6	1,1	0,1	2,5	1,4	1,2	2,1	0,4	8,2	6,6	10,6	nd	nd
PA7	18,5	0,0	2,9	3,1	0,4	2,4	> 45*	11,8	16,2	19,1	8,4	5,0
PA8	7,2	0,1	3,7	6,6	1,3	2,9	16,4	19,2	10,7	12,3	11,6	5,4
PA9	3,6	0,1	0,5	0,5	0,9	0,8	6,7	3,9	2,6	9,2	9,1	3,7
PL1	187,1	0,2	1,6	1,2	2,7	1,7	469,4	6,2	17,2	22,6	nd	nd
E1	mg/L	mg/L	mg/L	mg/L	mg/L	mg/L	mg/L	mg/L				
	152	14,4	131	5,9	133	400	113	2,8	13,6	12,3	nd	nd

\* lixiviate close to saturation with gypsum so that measured SO<sub>4</sub> contents are considered as minimum concentrations

Figure1  
[Click here to download high resolution image](#)

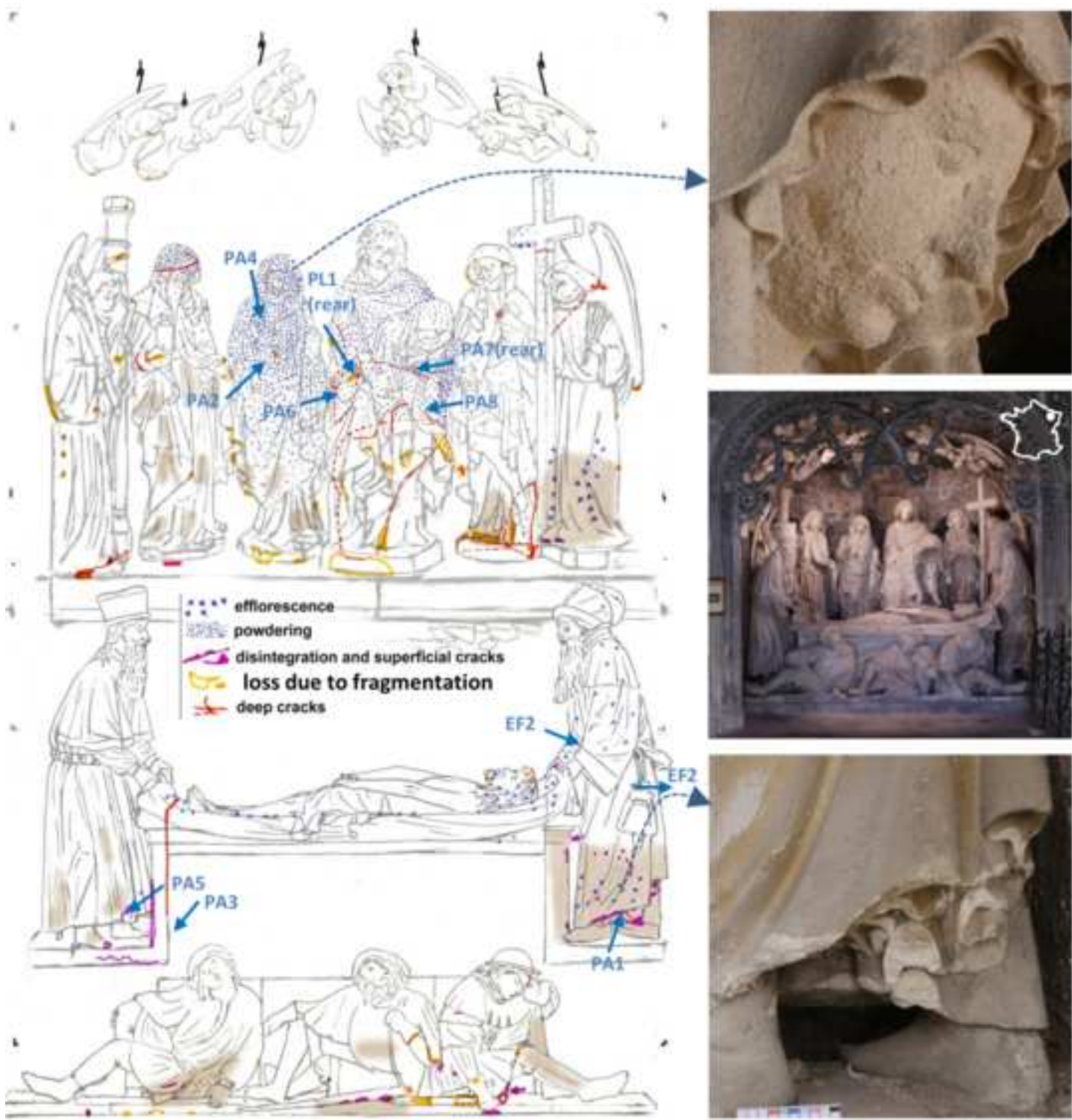


Figure2

[Click here to download high resolution image](#)

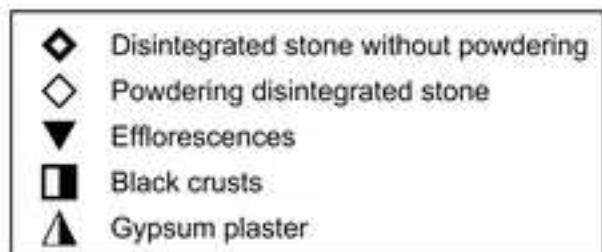
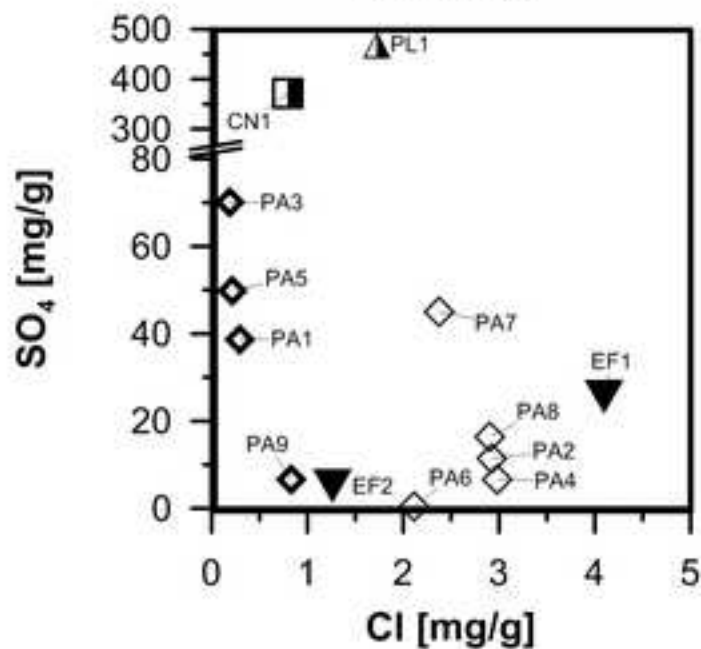
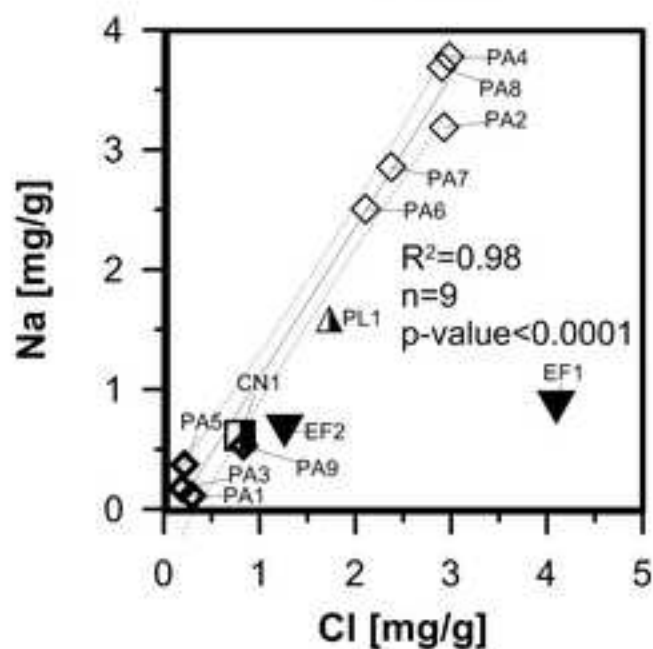
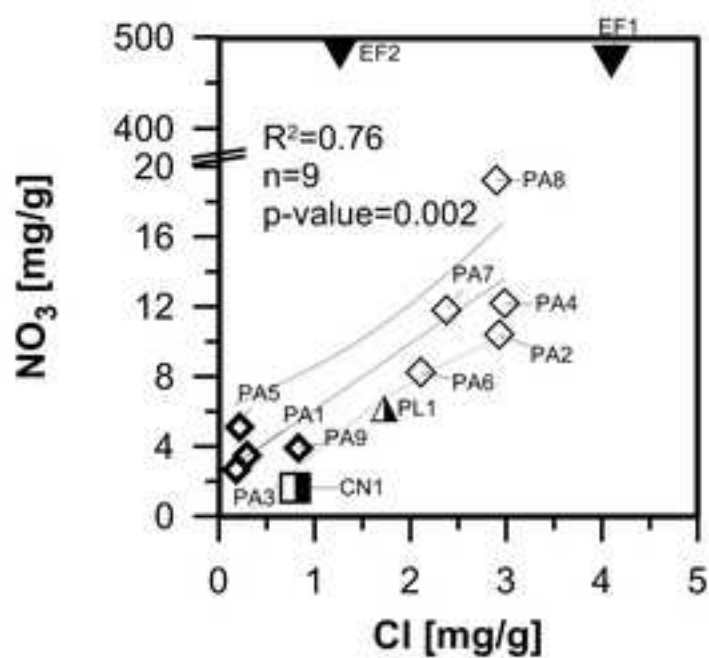
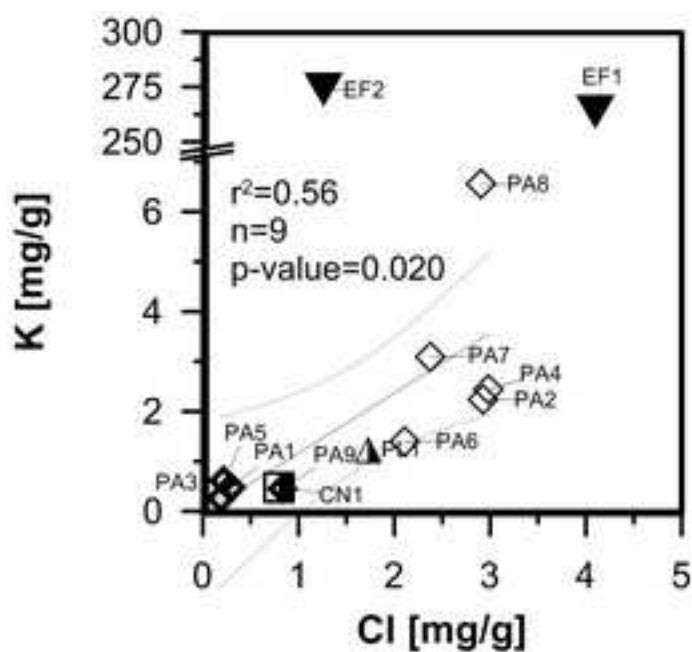


Figure3

[Click here to download high resolution image](#)

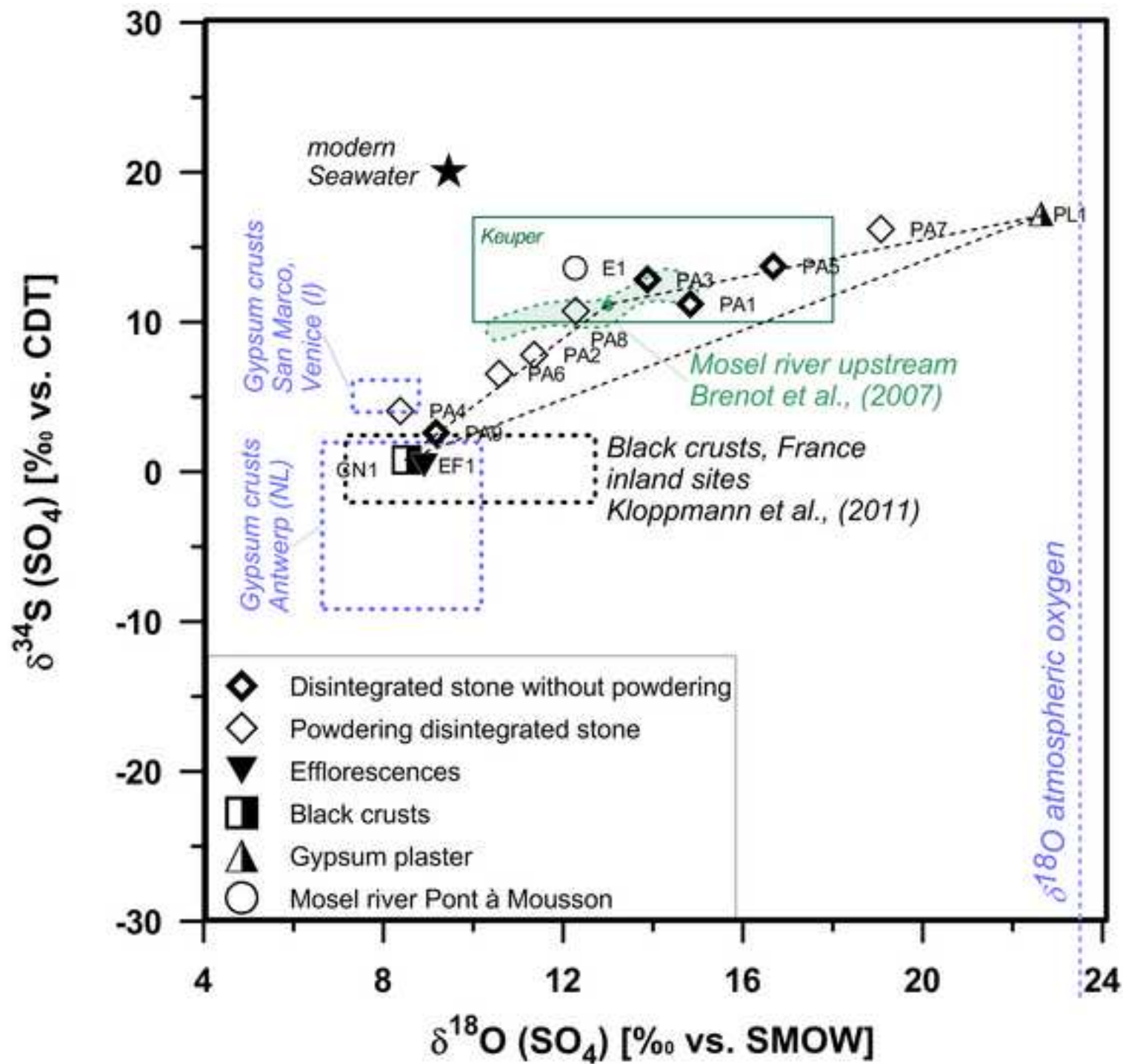
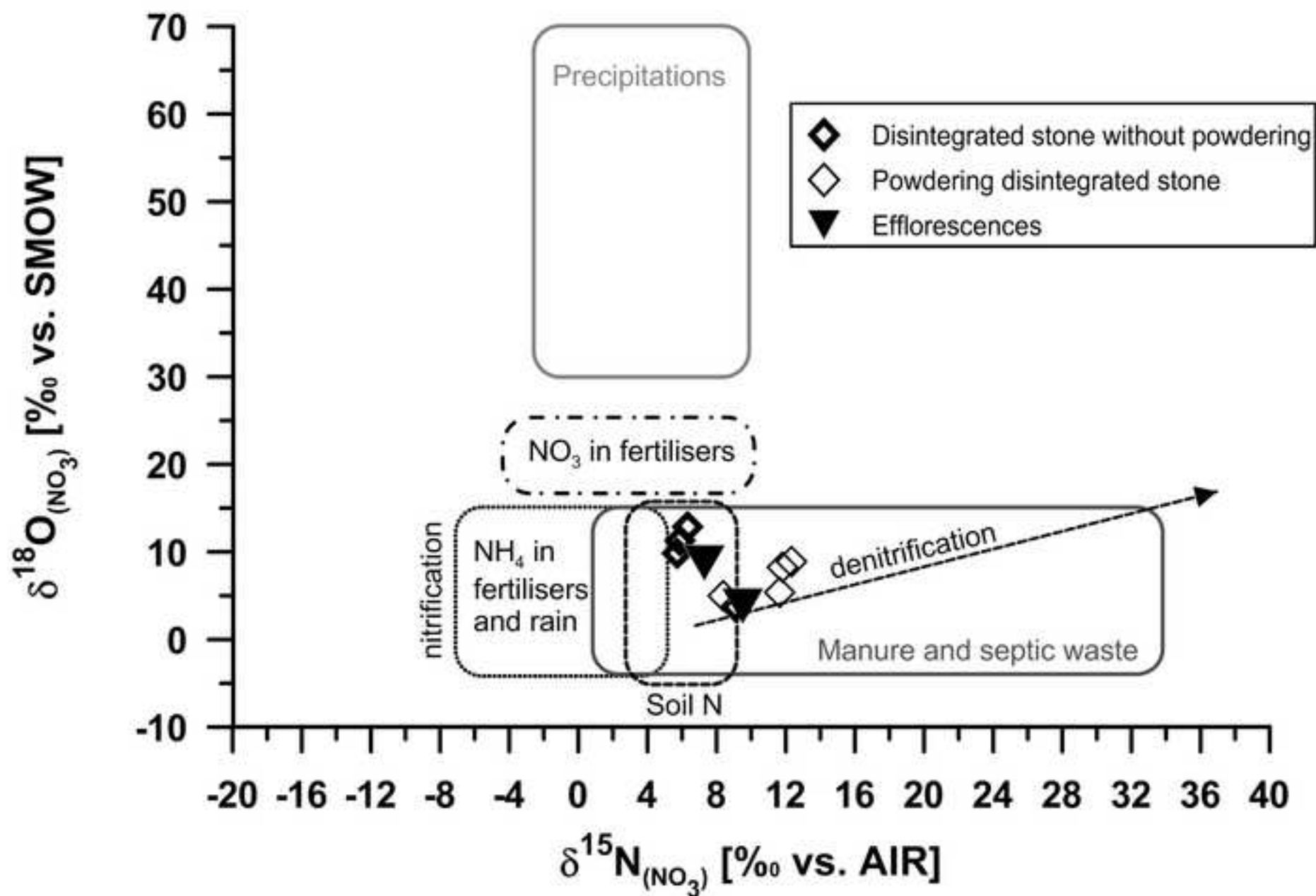




Figure4  
[Click here to download high resolution image](#)



**Supplementary Material**

[Click here to download Supplementary Material: Kloppmannet\\_al\\_STOTEN-D-12-03739R2-supplementary information.doc](#)